Journal of CO_2 Utilization 28 (2018) 299–305

Contents lists available at ScienceDirect

Journal of CO_2 Utilization

journal homepage: www.elsevier.com/locate/jcou

Tuning ionic liquids with imide-based anions for highly efficient CO_2 capture through enhanced cooperations

Yanjie Huang, Guokai Cui*, Huiyong Wang, Zhiyong Li, Jianji Wang*

Henan Key Laboratory of Green Chemistry, Collaborative Innovation Center of Henan Province for Green Manufacturing of Fine Chemicals, Key Laboratory of Green Chemical Media and Reactions, Ministry of Education, School of Chemistry and Chemical Engineering, Henan Normal University, Xinxiang, Henan, 453007, China

ARTICLE INFO

Keywords:
Ionic liquid
CO_2 capture
Anion
Cooperative interaction

ABSTRACT

Minimizing the release of CO_2 into the atmosphere is highly important due to the CO_2 concentration dependence of climate change. In this work, highly efficient capture of CO_2 is investigated through tuning ionic liquids (ILs) with imide-based anions. It is found that a superior high CO_2 capacity (2.21 mol mol^{-1}) be achieved by the imide-based IL with 1,2-cyclohexanedicarboximide anion at 20 °C and 1.0 bar through a combination of chemical and physical absorption. Quantum chemical calculations and spectroscopic analysis suggests that the significant increase in the CO_2 capacity is due to the enhanced cooperative interactions between CO_2 and three active sites in the anion with electron-donating group. Furthermore, the adsorbed CO_2 can be readily stripped from the CO_2-saturated IL through slightly heating or bubbling N_2, and the IL may be recycled without loss of efficiency.

1. Introduction

The increasing concentration of CO_2 in the atmosphere has triggered a series of inevitable problems, including greenhouse effect, ocean acidification, and the extinction of wildlife [1]. It is thus very important to decrease CO_2 emissions which mainly come from burning of the fossil fuels in power plants. The current industrial technology for CO_2 capture is using aqueous alkanolamine solutions [2,3]. However, the disadvantages of this method including high energy consumption and difficult regeneration/recycling should not be ignored [4–6]. Therefore, the development of new absorbents, which are highly efficient and reversible for CO_2 absorption, is a significant challenge.

Ionic liquids (ILs), especially functionalized ILs, have been used as alternative absorbents for efficient acid gas absorption for many years because of their unique physicochemical properties, such as high thermal stability, low vapor pressure, wide liquid temperature range, and tunable property [7–9]. Since Brennecke et al. [10] reported the solubility of CO_2 in an IL named 1-butyl-3-methylimidazolium hexafluorophosphate ([Bmim][PF_6]), numerous efforts have been devoted to the studies of physical solubility of CO_2 in this kind of liquid salts [11]. However, the physisorption capacity by these conventional ILs is low and far from the need for separation of CO_2 under atmospheric pressure. Davis et al. [12] found for the first time that the IL with amino-grafted cation could absorb about 0.5 mol CO_2 per mole IL at atmospheric pressure. Since anions play a key role in determining CO_2 solubility in ILs [13,14], many kinds of functionalized anions such as amino acids [15–17], azolates [18–21] and phenolates [22–24] have been developed and used in CO_2 capture and up to equimolar CO_2 capacity (anion:CO_2 = 1:1) has been achieved. Recently, nearly doubled CO_2 capacities (anion:CO_2 = 1:2) through cooperative interactions between functionalized anions and CO_2 have been reported by Wang et al. [25], Tao et al. [26] and Cui et al. [27] Can we further increase the capture capacity of CO_2 through tuning the anion-functionalized ILs to enhance the binding affinity between cooperative sites and CO_2? This is really attractive for the researchers in this field.

Herein, three kinds of imide-based anion-functionalized tri-*n*-butylethylphosphonium ([P_{4442}]) ILs were developed. Cycloalkyl group, a representative electron-donating group, and phenyl group, a representative electron-withdrawing group, were tethered to succinimide anion ([H-Suc]) to form 1,2-cyclohexanedicarboximide ([Cy-Suc]) and *o*-phthalimide ([Ph-Suc]) anions, respectively (see Fig. 1 for the chemical structures and abbreviations of these imide-based ILs). Compared with [P_{4442}][H-Suc] (1.85 mol CO_2 mol^{-1} IL), the CO_2 capacity of [P_{4442}][Cy-Suc] was as high as 2.21 mol mol^{-1}, while [P_{4442}][Ph-Suc] could only capture 1.40 mol CO_2 per mol of IL under ambient conditions. FT-IR and NMR studies indicate that the superior high CO_2 capture capacity was attributed to the enhanced cooperative interactions between CO_2 and three active sites in the anion with electron-donating

* Corresponding authors.
E-mail addresses: cuiguokai@htu.edu.cn (G. Cui), jwang@htu.cn (J. Wang).

https://doi.org/10.1016/j.jcou.2018.10.013
Received 1 August 2018; Received in revised form 6 October 2018; Accepted 17 October 2018
Available online 24 October 2018
2212-9820/ © 2018 Elsevier Ltd. All rights reserved.

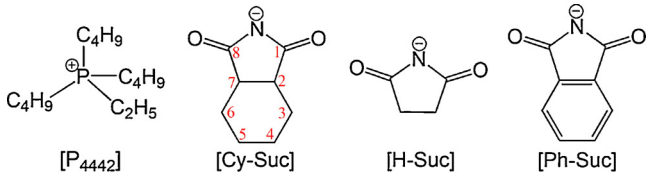

Fig. 1. Chemical structures and abbreviation of the cation and anions, where label of carbons in [Cy-Suc] was used for NMR analysis.

group.

2. Methods

2.1. Materials

Tri-*n*-butylphosphine (P_{444}), bromoethane, 1,2-cyclohexanedicarboximide (Cy-Suc), succinimide (H-Suc), and *o*-phthalimide (Ph-Suc) were obtained from Sigma-Aldrich. An anion-exchange resin (Amersep 900 OH) was supplied by Alfa Aesar. All these chemicals were used as received. CO_2 (99.999%) and N_2 (99.999%) were supplied by Beijing Oxygen Plant Specialty Gases Institute Co., Ltd. Mixed gases with different CO_2 partial pressure were prepared through mixing CO_2 with N_2 at different ratios.

2.2. Preparation of the ILs

$[P_{4442}][Br]$ was synthesized from P_{444} and bromoethane according to a slightly modified procedure reported in literature [28]. Bromoethane (1.20 g, 11 mmol) in acetonitrile (10 ml) was added dropwise into P_{444} (2.02 g, 10 mmol) in acetonitrile (10 ml) under ice-water conditions, and the mixture was slowly heated to 60 °C and stirred for 2 d. Then, acetonitrile was removed under reduced pressure at 70 °C, and the residue was washed with *n*-hexane (3 × 320 ml). The obtained solid was dried under reduced pressure at 80 °C for 1 d, and the final white solid product $[P_{4442}][Br]$ was obtained in a yield of more than 85%.

Imide-based ILs were synthesized through neutralization reaction between an ethanol solution of phosphonium hydroxide ($[P_{4442}][OH]$) and weak proton donors such as Cy-Suc, H-Suc and Ph-Suc. $[P_{4442}][OH]$ was prepared from $[P_{4442}][Br]$ through anion-exchange method [21]. In a typical procedure for the synthesis of $[P_{4442}][Cy\text{-}Suc]$, an ethanol solution of $[P_{4442}][OH]$ and equimolar 1,2-cyclohexanedicarboximide were mixed and stirred at room temperature for 24 h. After that, ethanol and produced water were evaporated at 60 °C under reduced pressure. The obtained ILs were dried under reduced pressure at 60 °C for 24 h to remove possible residual moisture.

2.3. Characterization of the ILs

NMR (Bruker 400 MHz) and FT-IR (Nicolet 4700) measurements were used to confirm the chemical structures of these imide-based ILs before and after the absorption of CO_2. The residual DMSO (2.50 ppm in the ^1H NMR and 39.52 ppm in the ^{13}C NMR spectrum) was used as the internal reference. Karl Fisher titrator (Mettler Toledo DL32) was used to determine the water content in these imide-based ILs, and less than 0.1 wt% of water was found. A Br^- selective electrode coupled with a saturated calomel electrode (Shanghai Precision & Scientific Instrument Co. Ltd) was used to measure the bromide content in these ILs, and it was found to be lower than 0.009 mol kg^{-1}. The density and viscosity of the imide-based ILs were also determined by an Anton Paar DMA 4500M densimeter and a Brookfield DV-II + Pro viscometer, respectively, at different temperatures.

2.4. CO_2 capture and release

CO_2 (flow rate: 60 ml min^{-1}) was bubbled through about 1.0 g IL in a glass container (inner diameter: 10 mm), which was partly immersed in a circulation water bath with desirable temperature. An electronic balance (accuracy: ± 0.0001 g) was used to determine the amount of absorbed CO_2 at regular intervals until equilibrium was reached. Desorption of CO_2 was carried out and monitored in an analogous way, and the ILs were regenerated by heating or bubbling N_2 through the CO_2-saturated ILs. In a typical desorption experiment, N_2 (flow rate: 60 ml min^{-1}) of atmospheric pressure was bubbled through about 1.0 g CO_2-saturated IL at 60 °C, and the amount of CO_2 release was determined at regular intervals by the electronic balance.

Table 1
Density (ρ) and viscosity (η) of the imide-based ILs at 20 °C.

IL	M (g mol^{-1})	ρ (g cm^{-3})	η (mPa s)
$[P_{4442}][Cy\text{-}Suc]$	383.56	1.0082	2567.0
$[P_{4442}][H\text{-}Suc]$	329.47	1.0198	998.0
$[P_{4442}][Ph\text{-}Suc]$	377.51	1.0750	127.4

3. Results and discussion

3.1. Density and viscosity

Considering the fact that physical properties may affect the stability and recycling performance of the ILs themselves as well as the mass transfer of CO_2, density (ρ) and viscosity (η) of the imide-based ILs were measured and the values at 20 °C were listed in Table 1. It shows that ρ and η values were greatly different for the studied ILs, where the density of $[P_{4442}][Cy\text{-}Suc]$ was the lowest but its viscosity was the highest. Values of ρ and η were also determined as a function of temperature (from 20 °C to 80 °C), and the results were included in Tables S1 and S2, respectively.

3.1.1. Temperature-dependent density

Fig. 2 shows a linear relationship between the density and the temperature, and the temperature dependence of density could be simply expressed by using Eq. (1):

$$\rho = a + bT \quad (1)$$

where ρ (in g cm^{-3}) is the density, a and b are constants, and T (in K) is the temperature. The values of a,b and the linear correlation coefficient r^2 were presented in Table 2.

3.1.2. Temperature-dependent viscosity

The effect of temperature on the viscosity of these imide-based ILs under atmospheric pressure was studied (Fig. 3). Clearly, the viscosity

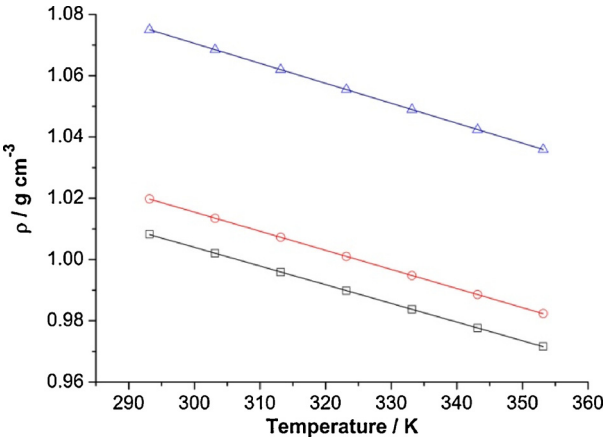

Fig. 2. Density of the imide-based ILs at different temperatures. $[P_{4442}][Cy\text{-}Suc]$, □; $[P_{4442}][H\text{-}Suc]$, ○; $[P_{4442}][Ph\text{-}Suc]$, △.

Table 2
Fitting parameters from the experimental densities of the prepared ILs.

IL	Parameter		
	a	b[$\times 10^4$]	r^2
[P_{4442}][Cy-Suc]	1.1871	−6.1036	0.99996
[P_{4442}][H-Suc]	1.2025	−6.2321	0.99999
[P_{4442}][Ph-Suc]	1.2662	−6.5214	1

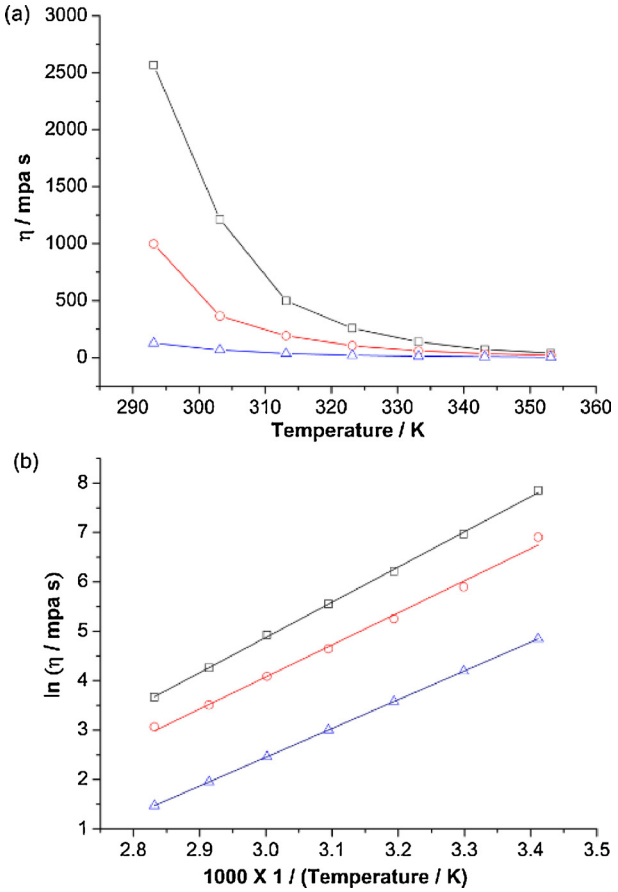

Fig. 3. Viscosity of the imide-based ILs at different temperatures (a), and the relationship between ln η and $1/T$ (b). [P_{4442}][Cy-Suc], □; [P_{4442}][H-Suc], ○; [P_{4442}][Ph-Suc], △.

was dramatically reduced with the increase of temperature from 20 °C to 80 °C (Fig. 3a). Such a change could be approximately fitted by Arrhenius Eq. (2):

$$\ln\eta = \ln A + E_\eta/RT \quad (2)$$

where η (in mpa s) represents the viscosity, E_η (in kJ mol^{-1}) is the flow activation energy, R is the universal gas constant (R = 8.314 J mol^{-1} K^{-1}) and A is the viscosity parameter. The fitting curves of ln η versus $1/T$ were shown in Fig. 3b. It is clear that ln η versus $1/T$ could be excellently correlated using the Arrhenius model. The fitted parameters A,E_η, and the correlation coefficient r^2 were listed in Table 3. The calculated E_η values for [P_{4442}][Cy-Suc], [P_{4442}][H-Suc] and [P_{4442}][Ph-Suc] were 60.1, 54.0 and 48.4 kJ mol^{-1}, respectively.

3.2. CO_2 capture

3.2.1. Effect of chemical structures of the ILs

The effect of chemical structures of these imide-based ILs on CO_2 capture was studied, and the absorption data were shown in Fig. 4. It

Table 3
Fitting parameters from the experimental viscosities of the prepared ILs.

IL	Parameter		
	E_η (kJ mol^{-1})	A[$\times 10^7$]	r^2
[P_{4442}][Cy-Suc]	60.1	0.5079	0.99916
[P_{4442}][H-Suc]	54.0	2.0458	0.99427
[P_{4442}][Ph-Suc]	48.4	3.0356	0.99998

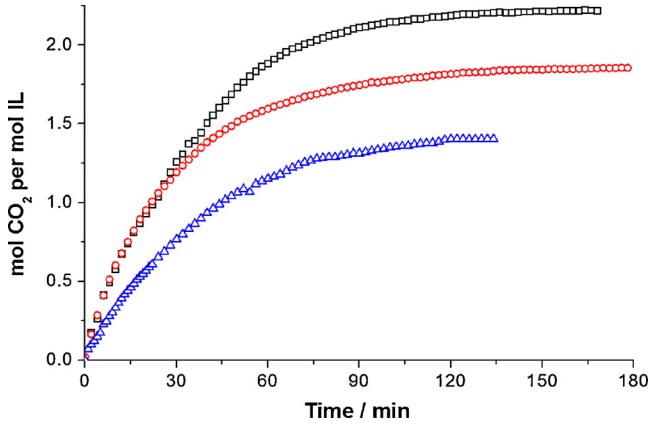

Fig. 4. CO_2 absorption by ILs as a function of absorption time at 20 °C and 1 bar. [P_{4442}][Cy-Suc], □; [P_{4442}][H-Suc], ○; [P_{4442}][Ph-Suc], △.

was found that CO_2 capacities of [P_{4442}][Cy-Suc], [P_{4442}][H-Suc] and [P_{4442}][Ph-Suc] were 2.21, 1.85 and 1.40 mol CO_2 per mole IL at 20 °C and 1.0 bar. Clearly, the absorption capacity of [P_{4442}][Cy-Suc] is much higher than that of other typical functionalized ILs, and this is the highest absorption capacity by ILs reported up to now (Table 4). In order to compare the interactions of CO_2 with active sites in [Cy-Suc], [H-Suc] and [Ph-Suc] anions, natural bond orbital (NBO) [29] charge distribution of N and O atoms in these anions was calculated using Gaussian 09 program [30] at the B3LYP/6-31 + + G(p,d) level [31–33]. As can be seen from Table S3, the NBO charge of N atom on [Cy-Suc], [H-Suc], and [Ph-Suc] was –0.686, –0.678, and –0.676, respectively, indicating that the electron-donating group increased but the electron-withdrawing group decreased the negative charge on the N active site. On the other hand, the electron-withdrawing group also caused a dramatic decrease in two C═O active sites. For example, the NBO charge of O atoms on the [H-Suc] and [Ph-Suc] was –0.701 and –0.661, respectively. Thus, the results indicate that the sites (O═C–N–C═O) on the [Cy-Suc] were more active than the same sites on the [Ph-Suc] in the capture of CO_2. These results also demonstrated that the CO_2 capacity could be efficiently improved through tuning of the cooperative

Table 4
Comparison of CO_2 absorption capacity among the ILs used in this work and other typical functionalized ILs reported in literatures.

IL	T (°C)	CO_2 Capacity (mol CO_2 / mol IL)	Reference
[P_{4442}][Cy-Suc]	20	2.21	This work
[P_{4442}][H-Suc]	20	1.85	This work
[P_{4442}][Ph-Suc]	20	1.40	This work
[P_{4442}][DAA]	20	1.25	[27]
[P_{4442}]$_2$[IDA]	40	1.69	[26]
[P66614][2-Op]	20	1.58	[25]
[MTBDH][TFE]	23	1.13	[37]
[P66614][Im]	23	1.00	[21]
[P66614][PhO]	30	0.85	[24]
[P66614][2-CN-Pyr]	22	~0.9	[18]
[P66614][Pro]	22	~0.9	[17]
[APbim][BF_4]	22	~0.5	[12]

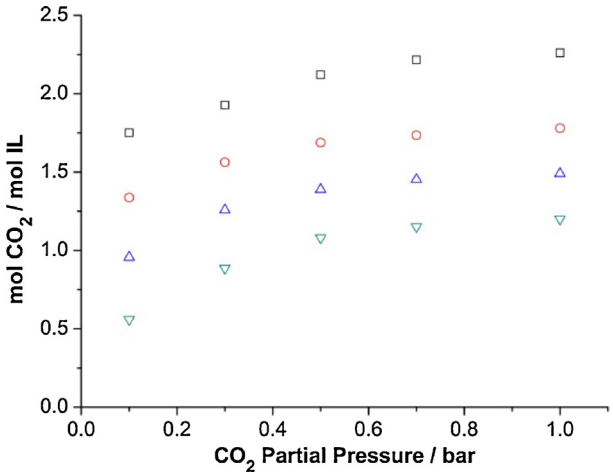

Fig. 5. Effect of CO_2 partial pressure and absorption temperature on the absorption performance of CO_2 by $[P_{4442}][Cy\text{-}Suc]$. 20 °C, □; 30 °C, ○; 40 °C, △; 50 °C, ▽.

interactions between CO_2 and imide-based anion by different substituents.

3.2.2. Effect of partial pressure and temperature

The effect of CO_2 partial pressure and absorption temperature on carbon capture by anion-functionalized IL $[P_{4442}][Cy\text{-}Suc]$ was also examined (Fig. 5). Although the CO_2 capacity by $[P_{4442}][Cy\text{-}Suc]$ was decreased from 2.21 to 1.76 mol CO_2 per mole IL with the CO_2 partial pressure decreased from 1.0 bar to 0.1 bar, the molar ratio of captured CO_2 to $[P_{4442}][Cy\text{-}Suc]$ is still higher than 1.5, indicating that CO_2 in flue gas (10–15 vol% CO_2) could be efficiently captured by these ILs. Moreover, the CO_2 capacity of $[P_{4442}][Cy\text{-}Suc]$ was reduced significantly with the increase of temperature. For instance, molar ratio of CO_2 to $[P_{4442}][Cy\text{-}Suc]$ was decreased from 2.21 to 1.20 with the absorption temperature increased from 20 to 50 °C under 1.0 bar of CO_2, which demonstrates that the captured CO_2 could be readily stripped from the CO_2-saturated $[P_{4442}][Cy\text{-}Suc]$ through slightly heating or bubbling N_2.

3.3. Regeneration of the ILs

Multiple CO_2 absorption-desorption cycles were studied by using $[P_{4442}][Cy\text{-}Suc]$ as an example, and the results were shown in Fig. 6. Clearly, the high CO_2 absorption capacity and rapid absorption rate were remained steady during the process of CO_2 absorption-desorption

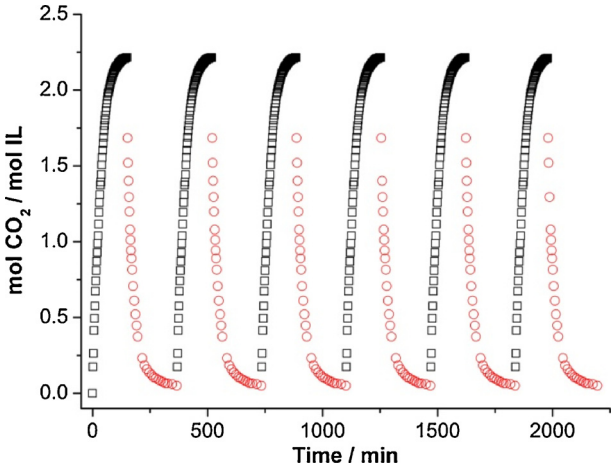

Fig. 6. Six cycles of CO_2 absorption and desorption by $[P_{4442}][Cy\text{-}Suc]$.

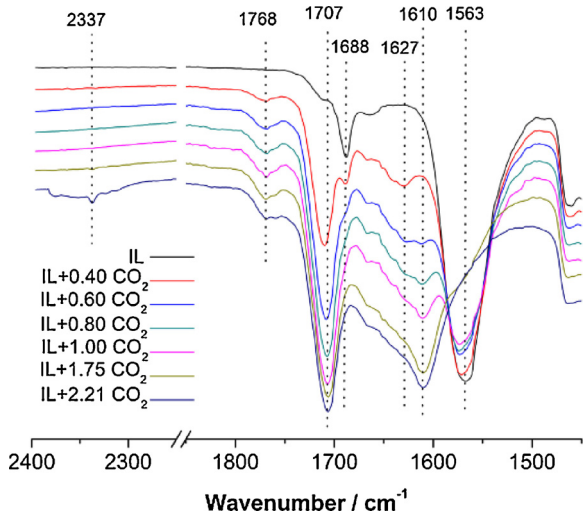

Fig. 7. FT-IR spectra of $[P_{4442}][Cy\text{-}Suc]$ with different absorption capacities of 100 vol% CO_2 (in mol mol^{-1}).

by $[P_{4442}][Cy\text{-}Suc]$, indicating that the absorption process was highly reversible and energy-saving.

3.4. The possible mechanism for CO_2 absorption

3.4.1. FT-IR analysis

FT-IR spectra of $[P_{4442}][Cy\text{-}Suc]$ before and after the absorption of CO_2 were shown in Fig. 7, and used to understand the cooperative interaction between imide-based anion [Cy-Suc] and CO_2. It can be seen that the bands at 1688 and 1563 cm^{-1}, which could be ascribed to cyclic imide anion, moved to 1768 and 1707 cm^{-1}, respectively, during the absorption of 100 vol% CO_2, implying the existence of strong chemical interactions between [Cy-Suc] anion and CO_2 [34]. When 0.40 mol CO_2 per mole IL was absorbed, a new peak was observed at 1627 cm^{-1}, which could be attributed to the asymmetrical stretching vibration of C═O in N−CO_2 resulted from N···CO_2 interaction between CO_2 and [Suc]. As the capacity was increased to 0.60 mol mol^{-1} CO_2, another new characteristic peak appeared at 1610 cm^{-1}, indicating the asymmetrical stretching vibration of C═O in O−CO_2 due to the N···CO_2···O interaction of CO_2 with N and O active sites. [24,27] The peak intensity at 1610 cm^{-1} gradually increased and the peak at 1627 cm^{-1} was then covered during the increase of CO_2 absorption capacity. These results indicate that: (1) the first stage of the CO_2 capture by the IL with [Cy-Suc] anion involved the N···CO_2 interaction, (2) the second stage included additional O···CO_2 interactions, and the interaction between CO_2 and N atoms was stronger than that of CO_2 and O atoms. Furthermore, a new peak at 2337 cm^{-1} could be observed in the IR spectrum of CO_2-saturated $[P_{4442}][Cy\text{-}Suc]$ (2.21 mol CO_2 per mol IL), suggesting the physical absorption of CO_2 by the anion. That is the third stage of CO_2 absorption by $[P_{4442}][Cy\text{-}Suc]$. Clearly, the interaction between CO_2 and the IL was mainly chemical when less than 2 mol CO_2 was captured by 1 mol $[P_{4442}][Cy\text{-}Suc]$, but the CO_2 absorption became physical when more than 2 mol CO_2 per mol IL was captured.

3.4.2. NMR analysis

^{13}C NMR and ^{1}H NMR spectra of $[P_{4442}][Cy\text{-}Suc]$ during the absorption of CO_2 were determined (Fig. 8). It is clearly noted that after the capture of CO_2 by $[P_{4442}][Cy\text{-}Suc]$, a signal appeared at 158–159 ppm in the ^{13}C NMR spectra. As the amount of absorbed CO_2 gradually increased, the intensity of this signal slightly increased and its position slowly shifted downfield. In detail, when $[P_{4442}][Cy\text{-}Suc]$ reacted with the first 0.8 mol mol^{-1} CO_2, the signal at 195.6 ppm for C═O in [Cy-Suc] anion was shifted quickly to 188.0 ppm due to the strong

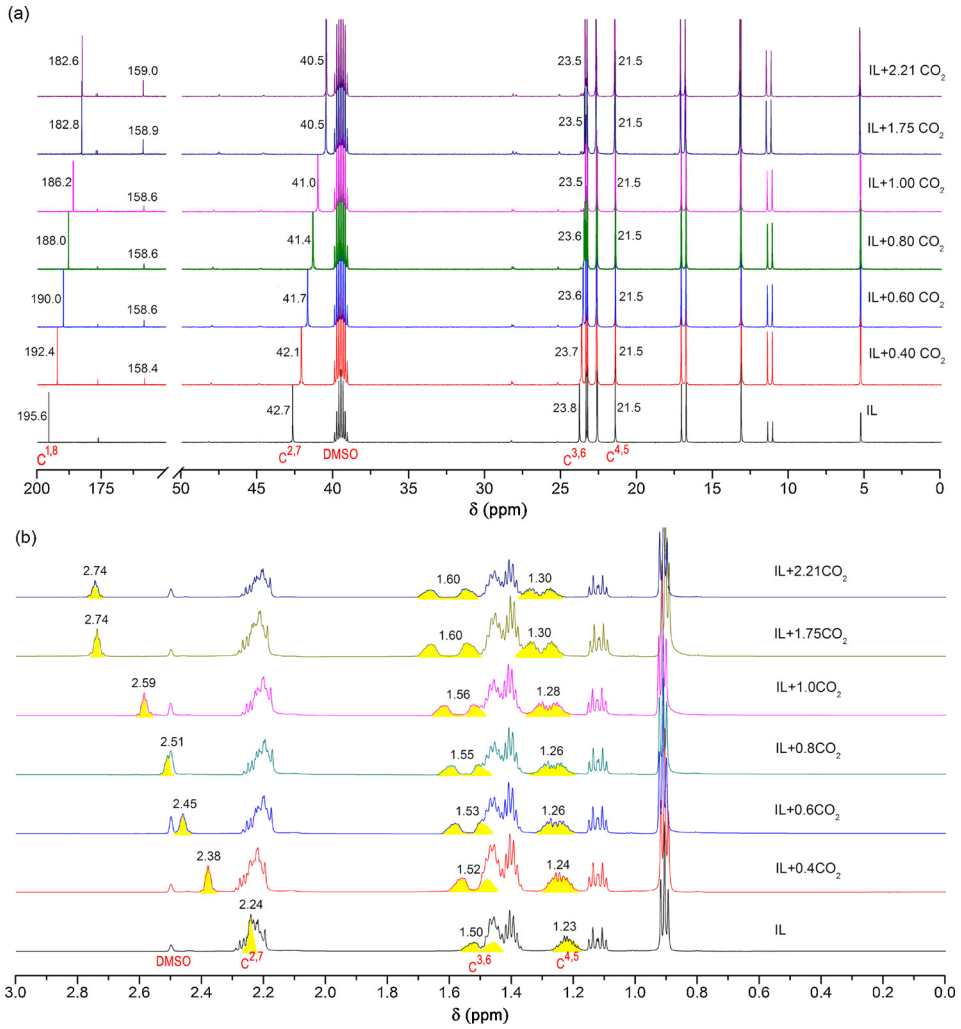

Fig. 8. ^{13}C NMR (a) and ^{1}H NMR (b) spectra of $[P_{4442}][Cy\text{-}Suc]$ with different absorption capacities of 100 vol% CO_2 (in mol mol^{-1}).

interaction between N atom and CO_2. This signal shifted slowly after 1.0 mol mol^{-1} CO_2 was captured, and was observed at 182.8 ppm when the IL reacted with another 0.95 mol mol^{-1} CO_2, suggesting the interactions between CO_2 and two C═O in the anion. Besides, the signal shift of C═O was only 0.2 ppm when another 0.46 mol mol^{-1} CO_2 was captured. This is a strong indication of physical interactions between CO_2 and anion. Additionally, the typical carbon signal of C4 and C5 at 21.5 ppm in the ^{13}C NMR spectra was not shifted, while the corresponding hydrogen signal in the ^{1}H NMR spectra was shifted downfield from 1.23 to 1.30 ppm during the uptake of CO_2, indicating the physical C—H···O hydrogen bond between methylene in the anion and O atom in the CO_2. Thereby, our results suggest that (1) the first stage was dominated by N···CO_2 interaction, (2) the second stage was dominated by additional O···CO_2 interactions, and (3) the third stage involved physical interaction, and the last interaction was weaker than the first two interactions.

Based on the previous reports [21,24,34,35] as well as the absorption results and the FT-IR and NMR analysis, the multiple-site mechanism of CO_2 (100 vol%) absorption by $[P_{4442}][Cy\text{-}Suc]$ could be proposed as follows (Fig. 9).

3.4.3. Quantum chemical calculations

Gaussian 09 program was also used to study the proposed multiple-site absorption mechanism in Fig. 9. In order to clearly show the interactions between CO_2 and multiple active sites on the anion, the calculations were performed through minimizing the geometries of the

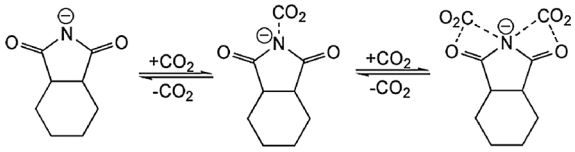

Fig. 9. Possible CO_2 absorption mechanism by $[P_{4442}][Cy\text{-}Suc]$ through multiple-site cooperative interactions.

complexes between [Cy-Suc] and CO_2. In detail, the geometry and energy optimization for each free CO_2 molecule, free anion and anion − CO_2 complex were calculated by dispersion corrected density functional theory (DFT-D3(BJ)) at the B3LYP/6-31 + + G(p,d) level. The optimized structures of [Cy-Suc] − CO_2 and [Cy-Suc]–2CO_2, reflecting the cooperative interactions between the active sites and CO_2, were shown in Fig. 10. It was found that the distance between negative-charged N atom in [Cy-Suc] anion and CO_2 molecule in [Cy-Suc] − CO_2 complex was 1.624 Å, indicating the N···CO_2 interaction. For [Cy-Suc]–2CO_2 complex, the distances between active sites in [Cy-Suc] anion and two CO_2 molecules were 2.851 and 2.853 Å for N···CO_2 and 2.854 and 2.854 Å for O···CO_2, respectively, which suggest that the multiple-site cooperation interaction in [Cy-Suc]–2CO_2 was weaker than single-site interaction in [Cy-Suc] − CO_2. We also calculated the enthalpies for the complex between [Cy-Suc] and CO_2. Although the enthalpies of [Cy-Suc] − CO_2 and [Cy-Suc]-2CO_2 complexes were only − 35.0 and − 34.6 kJ mol^{-1}, respectively, these results suggest that the desorption was easy at higher temperature and the proposed 1:2 CO_2

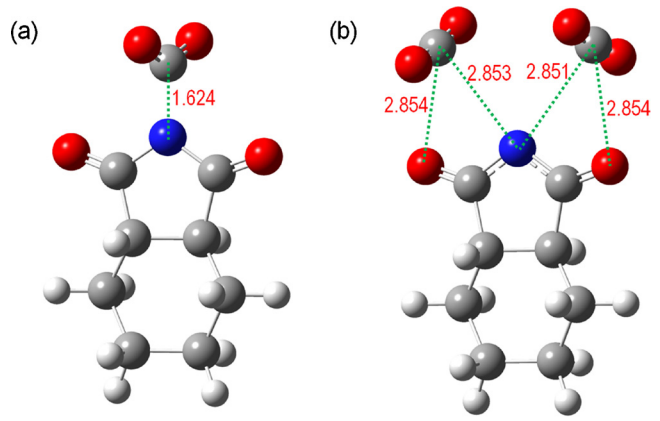

Fig. 10. Optimized structures of [Cy-Suc]−CO_2 (a) and [Cy-Suc]–2CO_2 (b) complexes at B3LYP/6-31 + + G(d,p) level. The van der Waals radii (in Å) are 1.70 (C), 1.20 (H), 1.52 (O), and 1.55 (N), respectively. [36] C, grey; H, white; O, red; N, blue.

multiple-site cooperation mechanism was reasonable. Further study is undergoing in our lab.

4. Conclusions

In this work, improvement of CO_2 absorption capacity was attempted by tuning ILs with imide-based anions through cooperative interactions between anion and CO_2. It was found that [P_{4442}][Cy-Suc] exhibited significant increase in CO_2 capacity, and up to 2.21 mol mol^{-1} CO_2 could be captured by IL at 20 °C and 1.0 bar. Indeed, this is the highest absorption capacity reported up to now. Quantum chemical calculations showed that such a high CO_2 capacity was originated from the enhanced cooperative interactions between CO_2 and cycloalkyl-tethered succinimide anion. Spectroscopic investigation suggested that the absorption process could be divided into three stages, including N···CO_2, N···CO_2···O, and physical interactions. We believe that the strategy developed in this work may be applied to design other new functionalized ILs and for highly efficient capture of acidic gases such as CO_2 and SO_2.

Acknowledgements

This work was supported by the National Natural Science Foundation of China (Nos. U1704251, 21733011), the National Key Research and Development Program of China (No. 2017YFA0403101), the Science Foundation for Excellent Young Scholars of Henan Normal University (No. 15YQ002), and the 111 project (No. D17007). The DFT calculations were supported by the High Performance Computing Center of Henan Normal University.

Appendix A. Supplementary data

Supplementary material related to this article can be found, in the online version, at doi:https://doi.org/10.1016/j.jcou.2018.10.013.

References

[1] S.J. Davis, K. Caldeira, H.D. Matthews, Future CO_2 emissions and climate change from existing energy infrastructure, Science 329 (5997) (2010) 1330–1333.
[2] B. Han, C. Zhou, J. Wu, D.J. Tempel, H. Cheng, Understanding CO_2 capture mechanisms in aqueous monoethanolamine via first principles simulations, J. Phys. Chem. Lett. 2 (6) (2011) 522–526.
[3] G.T. Rochelle, Amine scrubbing for CO_2 capture, Science 325 (5948) (2009) 1652–1654.
[4] S. Zeng, X. Zhang, L. Bai, X. Zhang, H. Wang, J. Wang, D. Bao, M. Li, X. Liu, S. Zhang, Ionic-liquid-based CO_2 capture systems: structure, interaction and process, Chem. Rev. 117 (14) (2017) 9625–9673.
[5] K.E. Gutowski, E.J. Maginn, Amine-functionalized task-specific ionic liquids: a mechanistic explanation for the dramatic increase in viscosity upon complexation with CO_2 from molecular simulation, J. Am. Chem. Soc. 130 (44) (2008) 14690–14704.
[6] X. Li, M. Hou, Z. Zhang, B. Han, G. Yang, X. Wang, L. Zou, Absorption of CO_2 by ionic liquid/polyethylene glycol mixture and the thermodynamic parameters, Green Chem. 10 (8) (2008) 879–884.
[7] D.L. Gin, R.D. Noble, Designing the next generation of chemical separation membranes, Science 332 (6030) (2011) 674–676.
[8] G. Cui, J. Zheng, X. Luo, W. Lin, F. Ding, H. Li, C. Wang, Tuning anion-functionalized ionic liquids for improved SO_2 capture, Angew. Chem. Int. Ed. 125 (40) (2013) 10814–10818.
[9] Z. Lei, C. Dai, B. Chen, Gas solubility in ionic liquids, Chem. Rev. 114 (2) (2014) 1289–1326.
[10] L.A. Blanchard, D. Hancu, E.J. Beckman, J.F. Brennecke, Green processing using ionic liquids and CO_2, Nature 399 (1999) 28.
[11] X. Huang, C.J. Margulis, Y. Li, B.J. Berne, Why is the partial molar volume of CO_2 so small when dissolved in a room temperature ionic liquid? Structure and dynamics of CO_2 dissolved in [$Bmim^+$] [PF_6^-], J. Am. Chem. Soc. 127 (50) (2005) 17842–17851.
[12] E.D. Bates, R.D. Mayton, I. Ntai, J.H. Davis, CO_2 capture by a task-specific ionic liquid, J. Am. Chem. Soc. 124 (6) (2002) 926–927.
[13] G. Cui, J. Wang, S. Zhang, Active chemisorption sites in functionalized ionic liquids for carbon capture, Chem. Soc. Rev. 45 (15) (2016) 4307–4339.
[14] J.L. Anderson, J.K. Dixon, J.F. Brennecke, Solubility of CO_2, CH_4, C_2H_6, C_2H_4, O_2, and N_2 in 1-Hexyl-3-methylpyridinium bis(trifluoromethylsulfonyl)imide: comparison to other ionic liquids, Acc. Chem. Res. 40 (11) (2007) 1208–1216.
[15] A.-H. Liu, R. Ma, C. Song, Z.-Z. Yang, A. Yu, Y. Cai, L.-N. He, Y.-N. Zhao, B. Yu, Q.-W. Song, Equimolar CO_2 capture by N-substituted amino acid salts and subsequent conversion, Angew. Chem. Int. Ed. 51 (45) (2012) 11306–11310.
[16] J. Zhang, S. Zhang, K. Dong, Y. Zhang, Y. Shen, X. Lv, Supported absorption of CO_2 by tetrabutylphosphonium amino acid ionic liquids, Chem. Eur. J. 12 (15) (2006) 4021–4026.
[17] B.E. Gurkan, J.C. de la Fuente, E.M. Mindrup, L.E. Ficke, B.F. Goodrich, E.A. Price, W.F. Schneider, J.F. Brennecke, Equimolar CO_2 absorption by anion-functionalized ionic liquids, J. Am. Chem. Soc. 132 (7) (2010) 2116–2117.
[18] B. Gurkan, B.F. Goodrich, E.M. Mindrup, L.E. Ficke, M. Massel, S. Seo, T.P. Senftle, H. Wu, M.F. Glaser, J.K. Shah, E.J. Maginn, J.F. Brennecke, W.F. Schneider, Molecular design of high capacity, low viscosity, chemically tunable ionic liquids for CO_2 capture, J. Phys. Chem. Lett. 1 (24) (2010) 3494–3499.
[19] G. Cui, N. Zhao, J. Wang, C. Wang, Computer-assisted design of imidazolate-based ionic liquids for improving sulfur dioxide capture, carbon dioxide capture, and sulfur Dioxide/Carbon dioxide selectivity, Chemistry 12 (21) (2017) 2863–2872.
[20] Y. Xu, CO_2 absorption behavior of azole-based protic ionic liquids: influence of the alkalinity and physicochemical properties, J. CO2 Util. 19 (2017) 1–8.
[21] C. Wang, X. Luo, H. Luo, D.-E. Jiang, H. Li, S. Dai, Tuning the basicity of ionic liquids for equimolar CO_2 capture, Angew. Chem. Int. Ed. 123 (21) (2011) 5020–5024.
[22] X.-M. Zhang, K. Huang, S. Xia, Y.-L. Chen, Y.-T. Wu, X.-B. Hu, Low-viscous fluorine-substituted phenolic ionic liquids with high performance for capture of CO_2, Chem. Eng. J. 274 (2015) 30–38.
[23] S. Ren, Y. Hou, S. Tian, X. Chen, W. Wu, What are functional ionic liquids for the absorption of acidic gases? J. Phys. Chem. B 117 (8) (2013) 2482–2486.
[24] C. Wang, H. Luo, H. Li, X. Zhu, B. Yu, S. Dai, Tuning the physicochemical properties of diverse phenolic ionic liquids for equimolar CO_2 capture by the substituent on the anion, Chem. Eur. J. 18 (7) (2012) 2153–2160.
[25] X. Luo, Y. Guo, F. Ding, H. Zhao, G. Cui, H. Li, C. Wang, Significant improvements in CO_2 capture by pyridine-containing anion-functionalized ionic liquids through multiple-site cooperative interactions, Angew. Chem. Int. Ed. 126 (27) (2014) 7173–7177.
[26] F.-F. Chen, K. Huang, Y. Zhou, Z.-Q. Tian, X. Zhu, D.-J. Tao, D.-E. Jiang, S. Dai, Multi-molar absorption of CO_2 by the activation of carboxylate groups in amino acid ionic liquids, Angew. Chem. Int. Ed. 55 (25) (2016) 7166–7170.
[27] Y. Huang, G. Cui, Y. Zhao, H. Wang, Z. Li, S. Dai, J. Wang, Preorganization and cooperation for highly efficient and reversible capture of low-concentration CO_2 by ionic liquids, Angew. Chem. Int. Ed. 129 (43) (2017) 13478–13482.
[28] G. Cui, C. Wang, J. Zheng, Y. Guo, X. Luo, H. Li, Highly efficient SO_2 capture by dual functionalized ionic liquids through a combination of chemical and physical absorption, Chem. Commun. 48 (20) (2012) 2633–2635.
[29] E.D. Glendening, A.E. Reed, J.E. Carpenter, F. Weinhold, NBO (Version 3.1), Theoretical Chemistry Institute, University of Wisconsin, Madison, 1998.
[30] M.J. Frisch, G.W. Trucks, H.B. Schlegel, G.E. Scuseria, M.A. Robb, J.R. Cheeseman, G. Scalmani, V. Barone, B. Mennucci, G.A. Petersson, H. Nakatsuji, M. Caricato, X. Li, H.P. Hratchian, A.F. Izmaylov, J. Bloino, G. Zheng, J.L. Sonnenberg, M. Hada, M. Ehara, K. Toyota, R. Fukuda, J. Hasegawa, M. Ishida, T. Nakajima, Y. Honda, O. Kitao, H. Nakai, T. Vreven, J.A.J. Montgomery, J.E. Peralta, F. Ogliaro, M. Bearpark, J.J. Heyd, E. Brothers, K.N. Kudin, V.N. Staroverov, T. Keith, R. Kobayashi, J. Normand, K. Raghavachari, A. Rendell, J.C. Burant, S.S. Iyengar, J. Tomasi, M. Cossi, N. Rega, J.M. Millam, M. Klene, J.E. Knox, J.B. Cross, V. Bakken, C. Adamo, J. Jaramillo, R. Gomperts, R.E. Stratmann, O. Yazyev, A.J. Austin, R. Cammi, C. Pomelli, J.W. Ochterski, R.L. Martin, K. Morokuma, V.G. Zakrzewski, G.A. Voth, P. Salvador, J.J. Dannenberg, S. Dapprich, A.D. Daniels, O. Farkas, J.B. Foresman, J.V. Ortiz, J. Cioslowski, D.J. Fox, Gaussian 09 (Revision D.01), Gaussian, Inc., Wallingford CT, 2013.
[31] A.D. Becke, Density-functional exchange-energy approximation with correct asymptotic behavior, Phys. Rev. A 38 (6) (1988) 3098–3100.
[32] C. Lee, W. Yang, R.G. Parr, Development of the Colle-Salvetti correlation-energy

formula into a functional of the electron density, Phys. Rev. B 37 (2) (1988) 785–789.
[33] A.D. Becke, Density-functional thermochemistry. 3. The role of exact exchange, J. Chem. Phys. 98 (7) (1993) 5648–5652.
[34] S. Zhang, Y.-N. Li, Y.-W. Zhang, L.-N. He, B. Yu, Q.-W. Song, X.-D. Lang, Equimolar carbon absorption by potassium phthalimide and in situ catalytic conversion under mild conditions, ChemSusChem 7 (5) (2014) 1484–1489.
[35] C. Cadena, J.L. Anthony, J.K. Shah, T.I. Morrow, J.F. Brennecke, E.J. Maginn, Why is CO_2 so soluble in imidazolium-based ionic liquids? J. Am. Chem. Soc. 126 (16) (2004) 5300–5308.
[36] A. Bondi, Van der waals volumes and Radii, J. Phys. Chem. 68 (3) (1964) 441–451.
[37] C. Wang, H. Luo, D.-E. Jiang, H. Li, S. Dai, Carbon dioxide capture by superbase-derived protic ionic liquids, Angew. Chem. Int. Ed. 49 (34) (2010) 5978–5981.